Supporting Information

Recyclable, Hybrid filler/PVA Nanocomposite Films with Enhanced Hydrophobic, Barrier, UV-resistance and Flame-retardant properties for Packaging Applications

V. Bavya [a,b], Harikrishnan P. S.[a], Rajan T.P.D.[a,b]* and Suresh K.I.[a,b,]*

[a] Materials Science and Technology Division, CSIR- National Institute for Interdisciplinary Science and Technology, Pappanamcode, Thiruvananthapuram - 695019, Kerala, India.

[b] Research Centre, University of Kerala, Thiruvananthapuram - 695034, Kerala, India.
*Corresponding author; E-mail: kisuresh@niist.res.in, tpdrajan@niist.res.in

QY measurement

The quantum yield (QY) of the prepared PCDs was determined using quinine sulfate as the reference standard (QY = 54%). Measurements were performed by comparing the fluorescence emission intensities and absorbance values of the PCD aqueous solution with those of quinine sulfate dissolved in 0.1 M H_2SO_4 (refractive index, η = 1.33). The QY was calculated according to Eq. (**S1**):

$$Q_S = Q_R * (I_S/I_R) * (A_R/A_S) * (\eta_S/\eta_R)^2 \text{----------Eq. (S1)}$$

Where Q denotes quantum yield, η and I are the solvent's refractive index and fluorescence intensity, respectively. A is the absorbance of CDots at the excitation wavelength, and Q_R is the quinine sulfate quantum yield in 0.1 M of H_2SO_4 solution (54 %). The subscripts S and R refer to the sample and references, respectively.

DPPH assay

The antioxidant activity was evaluated using the DPPH (2,2-diphenyl-1-picrylhydrazyl) radical scavenging assay. For the analysis, 0.05 g of the sample was mixed with 4 mL of a 100 μM DPPH solution, and the mixture was incubated for 30 min at room temperature. The absorbance was then recorded at 517 nm using a Shimadzu UV–Vis spectrophotometer. A DPPH solution without the sample served as the control. The antioxidant activity (%) was determined using the following expression[1]:

$$Free\ radical\ scavenging\ activity(\%) = \frac{A_0 - A_S}{A_0} * 100 \text{ ---------- Eq.(S2)}$$

Table S1: Gravimetric loading of phosphorus-doped carbon dots (PCD) onto porous silica

Sample Code	Mass of PS(g)	PCD Added (g)	MassAfter Loading (g)	Observation
PCD@HPS-0.5	1.00	0.50	1.48	No visible leaching
PCD@HPS-1	1.00	1.00	1.96	No visible leaching
PCD@HPS-1.5	1.00	1.50	2.43	No visible leaching
PCD@HPS-2	1.00	2.00	2.91	No visible leaching (Optimal)
PCD@HPS-2.5	1.00	2.50	2.95	Slight visible leaching observed
PCD@HPS-3	1.00	3.00	2.97	Visible leaching observed

Thickness of the film

The thickness of the films was measured using a digital screw gauge. Measurements were taken at 5 different locations on each film and averaged to ensure accuracy.

Optical Properties of the Films

The optical properties of the composite films were analyzed in terms of lightness (L*), red-green coordinate (a*), and yellow-blue coordinate (b*) using a HunterLab colorimeter, employing a standard white plate as the reference background. The total color difference (ΔE), whiteness index (WI), yellowness index (YI), and film transparency were calculated according to Equations (S3)-(S5). In these calculations, ΔL, Δa, and Δb correspond to the differences in L*, a*, and b* values of the composite films relative to the neat PVA film. For accuracy, each formulation was tested using three independent samples, and the average values were reported. The transparency of the films was determined using Equation (S6).

$$\Delta E = \sqrt{(\Delta L^*)^2 + (\Delta a^*)^2 + (\Delta b^*)^2}$$ ---------- **Eq.(S3)**

$$WI = 100 - \sqrt{(100 - L^*) + a^{*2} + b^{*2}}$$ ---------- **Eq. (S4)**

$$YI = 142.86 * b^*/L^*$$ ---------- **Eq.(S5)**

$$Transparency = \frac{-logT_{600}}{D}$$ ---------- **Eq.(S6)**

Water Resistance Analysis of the Films

The water absorption behavior of the composite films was assessed following ASTM D570-98 guidelines[2]. Pre-dried film specimens were immersed in 20 mL of distilled water at room temperature (25 °C). At 24 h intervals, the films were withdrawn, carefully blotted with a clean cloth to remove excess surface water, and weighed. The water absorption percentage was calculated using the equation:

Water absorption (%)=(W_{wet}-W_{dry})/W_{dry} *100%---------- Eq.(S7)

where W_{wet} represents the weight of wet film and W_{dry} represents the weight of dry film.

The water solubility (WS) of the films was determined as the relative weight loss of the samples upon immersion. For this, pre-dried films were immersed in distilled water and incubated at 25 °C for 24 h in a water bath shaker set at 100 rpm. After incubation, the undissolved residues were separated by filtration, dried at 100 °C for 24 h, and weighed[3]. The WS was then calculated using the following expression:

Water solubility (%)=(W_1-W_2)/W_1 *100%---------- Eq.(S8)

where W_1 and W_2 are the initial weight and the weight after treatment, respectively.

Barrier Properties of Films

The oxygen transmission rate (OTR) of the prepared films was evaluated using an OTR-1903 Oxygen Permeability Tester (ATIS-AT-1903, India), employing the coulometric sensor technique. The measurements were performed at 23 ± 1 °C and 0% relative humidity, and the OTR values were reported in cc/(m^2 . day). The water vapor transmission rate (WVTR) was

measured following the ASTM E96 procedure with the desiccant method. For this, films with a diameter of 5 cm were mounted onto the lids of Mason jars containing a pre-weighed desiccant. The jars were then sealed and were placed in a controlled environmental chamber maintained at 25 ± 2 °C and 70 ± 5% relative humidity, and the progressive weight gain attributed to water vapor permeating through the film and subsequently absorbed by the desiccant was monitored over time. WVTR was calculated g/ m^2 day using the following expression:

$$WVTR = \frac{k}{Permeation\ area} \text{ ---------- Eq.(S9)}$$

where *k* is the slope of water gain versus time. All measurements were performed in triplicates.

Dynamic Contact Antibacterial Assay

The dynamic contact antibacterial activity of the prepared films was evaluated using the shaking flask method, as described by Liu et al[4]. Prior to the experiment, all culture media, buffers, glassware, and instruments were sterilized by autoclaving at 121 °C for 15 min. *Staphylococcus aureus* (Gram-positive) and *Escherichia coli* (Gram-negative) were cultivated in sterile lysogeny broth (LB, 25 g L^{-1}) and incubated overnight at 37 °C with shaking at 200 rpm. The resulting bacterial cultures were then diluted with sterile phosphate-buffered saline (PBS, pH 7.2) to obtain a final optical density (OD) of 0.04.

Subsequently, 30 mg of each dried and sterilized film samples was introduced into sterile test tubes containing 3 mL of the prepared bacterial suspension. The tubes were incubated at 37 °C with continuous shaking at 200 rpm to maintain constant interaction between the film surfaces and the bacterial cells. After 3 h of incubation, 100 µL aliquots were withdrawn from each tube, spread evenly onto LB agar plates, and further incubated at 37 °C for 24 h to allow colony formation. The antibacterial performance of the films was determined by calculating the percentage of bacterial growth inhibition using the following equation:

$$Growth\ inhibition(\%) = \frac{A - B}{A} * 100 \text{ ----- Eq.(S10)}$$

where A represents the number of bacterial colonies in the control sample and B corresponds to the number of colonies observed in the presence of the film samples.

Migration Tests

The overall migration behavior of the nanocomposite films was evaluated gravimetrically following the procedure specified in European Union Commission Regulation (EU) No. 10/2011. Two food simulants were selected to represent different food environments: 10% (v/v) ethanol solution, simulating hydrophilic foods, and 3% (w/v) acetic acid solution, representing acidic food conditions. Film specimens with an area of approximately 1 dm^2 were immersed in glass bottles containing 100 mL of the respective food simulant. The bottles were tightly sealed and stored in a hot air oven at 40 °C for 10 days. After 10 days the bottles were removed from the oven and allowed to cool to room temperature. The film samples were then carefully removed from the simulant solutions. Subsequently, the simulant solutions were evaporated, and the remaining residues were dried at 105 °C overnight. After cooling to room temperature, the dried residues were weighed using an analytical balance. The overall migration values were calculated and expressed in mg/kg of food simulant. The obtained migration results were compared with the overall migration limit (OML) of 60 mg/kg established by EU Commission Regulation (EU) No. 10/2011 to assess the suitability of the films for food packaging applications[5].

Reprocessability Studies of Films

For reprocessability evaluation, the films were cut into small fragments and dissolved in deionized water at 95 °C for 2 h. The obtained solution was subsequently recast into Petri dishes and dried at 50 °C for 24 h. This reprocessing cycle was repeated five times[6]. After the 1^{st} and 5^{th} cycles, the mechanical properties of the regenerated films were measured to examine the retention of their functional performance.

Degradation test

Soil burial degradation of the films was assessed following a previously reported procedure. Initially, the films were oven-dried and weighed. The dried samples were then buried at a depth of 10 cm in compost soil, with moisture maintained by periodically adding 10 mL of water. After predetermined intervals, the films were retrieved, rinsed with water, and dried in an oven for 24 h. The samples were reweighed, and the percentage weight loss was calculated to estimate the degradation rate[7]. In addition, FTIR spectra were recorded weekly to monitor

structural and chemical changes during degradation, while SEM analysis was carried out after four weeks to examine surface morphological alterations.

Assessment of Fresh Fruit Packaging Efficiency

To evaluate the biological activity of the fabricated films, freshly harvested strawberries were placed in plastic boxes and sealed using the improvised packaging system, ensuring minimal direct exposure of the fruit surface to air. The packaged samples were stored at room temperature for 8 days. Imaging was carried out on the 0th, 2nd, 4th, 6th, and 8th days of storage at 25 ± 2 °C and in 70 ± 5% relative humidity. Throughout the storage period, key quality parameters, including weight loss, freshness, and organic acid content, were systematically monitored and analyzed[3].

Weight Loss Rate

The weight loss of strawberries was monitored to assess the effectiveness of the packaging films in maintaining fruit freshness during storage. The procedure followed a standard method reported in the literature[8]. Initially, the fresh strawberries were weighed to determine the initial weight (W_0) of each sample group. The samples were then stored under controlled conditions (26 °C and 37% relative humidity), and their weights (W_t) were recorded at predetermined time intervals. Prior to each measurement, the strawberries were carefully removed from the packaging, and any visible surface moisture was gently wiped off. The weights were measured using a digital balance with an accuracy of four decimal places. The percentage weight loss was calculated using the following expression[3]:

$$\text{Weight loss } (\%)=(W_0-W_t)/W_0 *100\% \quad \text{Eq.(S10)}$$

This percentage represents the extent of moisture loss during storage and serves as an indicator of the freshness and shelf life of the fruit. A lower weight loss corresponds to improved moisture retention, demonstrating the effectiveness of the packaging films in preserving the quality of strawberries.

Organic Acid Content

The organic acid content was measured according to the GB/T 12456-2008 protocol. Briefly, samples from each group were homogenized and combined with 100 mL of water preheated to 80 °C. The mixture was then brought to a boil for 30 min with gentle stirring, after which an additional amount of water at a temperature of 80 °C was added to adjust the total volume to

250 mL. The resulting suspension was filtered to remove solids, and a 25 mL aliquot of the filtrate was taken for titration in a 100 mL conical flask using 0.05 M NaOH. A blank titration was performed using 25 mL of distilled water. The organic acid content, expressed as malic acid equivalents, was calculated using the following equation[3]:

$$Organic\ acid\ content = \frac{(V - V_0) * .05 * 10 * .067}{W} * 100\% \quad \text{--------Eq.(S11)}$$

Here, V_0 and V (mL) are the amounts of 0.05 M NaOH used in the blank and experimental groups, respectively. W (g) is the total mass of samples. 0.067 is the conversion coefficient of malic acid.

Color Analysis

Hunter Lab Color Flex EZ Colorimeter (Hunter Associates Laboratory Inc., Reston) is used to measure the color of the fruit samples based on the L*, a*, and b* color systems. The "L*" value indicates the brightness, with 0-100 representing dark to light. The "a*" value gives the degree of the red-green color, and the "b*" value indicates the degree of the yellow-blue color. The samples were transferred into the cuvette and placed in the port after being standardized. The color values were noted with five rotations of each sample in triplicate.

Texture Analysis

TA1 Texture Analyzer (Lloyd Instruments, UK) with a 50kg load cell is used investigate the hardness of the strawberry samples. The probe was compressed until it penetrated 10 mm under the sample surface at a speed of 1 mm/s.

Flame retardancy

For the preliminary analysis of the flammability properties of the aerogels, vertical burning tests were conducted under laboratory conditions using a Bunsen burner with a butane flame. Limiting oxygen index (LOI), i.e., the lowest concentration of oxygen required to burn a sample, was measured for the films using a critical oxygen index apparatus (as per ASTM D2863-08) from Spectrum Automation and Controls, coupled with Servomex Servoflex MiniMP (United Kingdom), a high-performance oxygen gas analyzer

Cone calorimetry test

The cone calorimetry test was carried out using a FTT iCone classic cone calorimeter. The sample (105 mm* 105 mm *3 mm) was tested under N_2 and standard gas (CO, CO2, O2) atmospheres at a heat radiation Low rate of 35 kW m^2 and a cone temperature of 750 °C according to the test standard ISO 5660 and ASTM E1354

Other characterizations

The morphology and particle size of PCD were analyzed using a JEOL JEM-2010 electron microscope (JEOL, Japan) at an accelerating voltage of 300 kV. For TEM analysis, the PCD dispersion was drop-cast on carbon-coated type-B copper grids and dried under vacuum. The images were analyzed using Gatan and ImageJ software. The IR spectra of the samples were measured using a Spectrum Two FTIR spectrophotometer from M/S. PerkinElmer. Powder X-ray diffraction (PXRD) pattern samples were measured over a broad range of 2θ values ($10° < 2\theta < 80°$) using a PC-controlled Malvern PANalytical B V EMPYREAN 3 diffractometer with Ni-filtered Cu Kα radiation (45 kV, 40 mA, λ = 1.5406 Å). XPS data were acquired using a PHI 5000 Versa Probe-II Focus XPS (ULVAC-PHI Inc., USA) instrument equipped with a microfused (200 μm, 15 kV) monochromatic Al Kα X-ray source (hυ = 1486.6eV) and fitted using multipack software. Scanning Electron Microscopy (SEM), a Zeiss EVO 18 cryo-SEM at an accelerating voltage of 20 kV, is used to study the morphology of the films. Zeta potential measurements were conducted for the aqueous solutions of carbon dots using a Zetasizer (Nano ZS ZEN 3600, Malvern Instrument, UK). Specific surface area and porosity were studied by standard N_2 adsorption technique using Tristar II, Micromeritics surface area analyzer after degassing the samples at 150 ^oC for 2 h. Brunauer-Emmett-Teller (BET) model was utilized to calculate the specific surface areas. A desorption isotherm was used to determine the pore-size distribution using the Barrett-Joyner-Halenda (BJH) model. Thermogravimetric analysis (TGA) was carried out using a PerkinElmer STA6000 system under a nitrogen atmosphere, with a heating rate of 10 °C min^{-1} from 50 to 900 °C to assess thermal stability and decomposition behavior and Q20, TA instrument, USA was used for DSC. The optical absorption/emission properties were measured in a quartz cuvette. The emission spectra were recorded at room temperature using a SPEX-Fluorolog-3 FL3-221 spectrofluorimeter. The UV−vis spectra were recorded on a Shimadzu UV-2600 ultraviolet−visible absorption spectrometer. Time-correlated single photon counting (TCSPC) was carried out for analysis of fluorescence decay using a single picosecond photon counting system from M/S. Horiba,

DeltaFlex employs a 330 nm nano LED source as the excitation light. Tensile properties were conducted using a universal testing machine (Instron 3382, UK), as per ASTM-D-882 standard. Film hardness was determined using a Shore D durometer (STECH Engineers) in accordance with ASTM D2240-15. A moisture analyzer (Aczet Model) was used to determine the moisture content of samples at 110 °C (IR source).

Results and Discussion

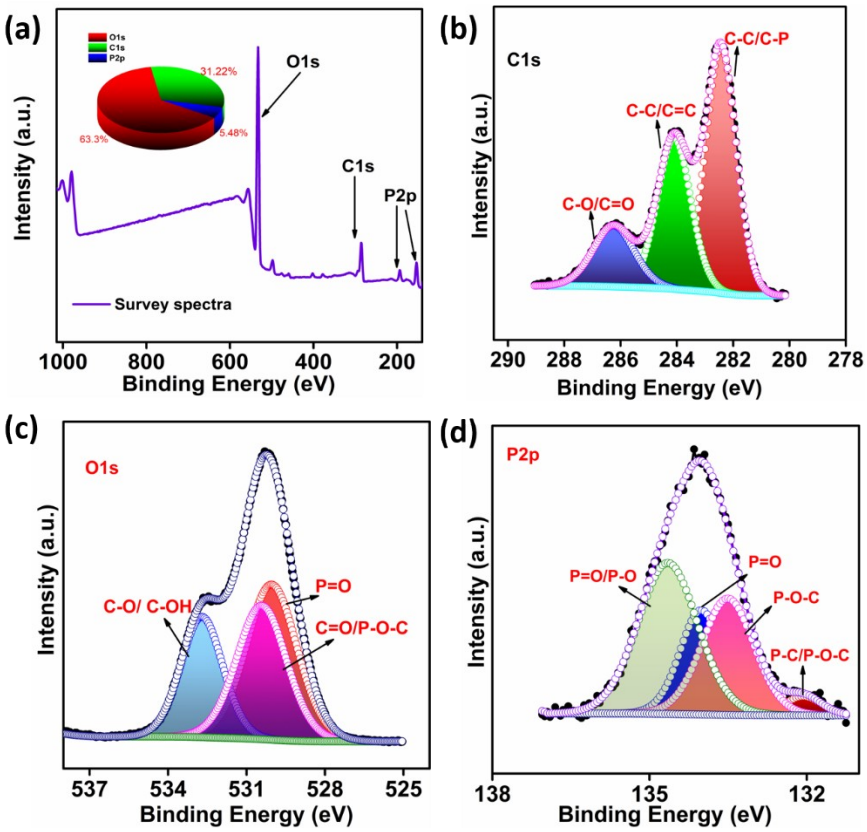

Figure S1: XPS (a) survey spectra and deconvoluted (b) C1s, (c) O1s, and (d) P2p of PCD

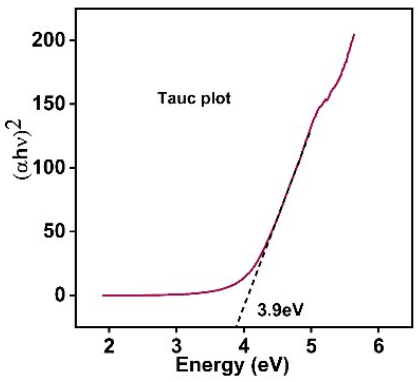

Figure S2: Tauc plot from UV analysis

(i)

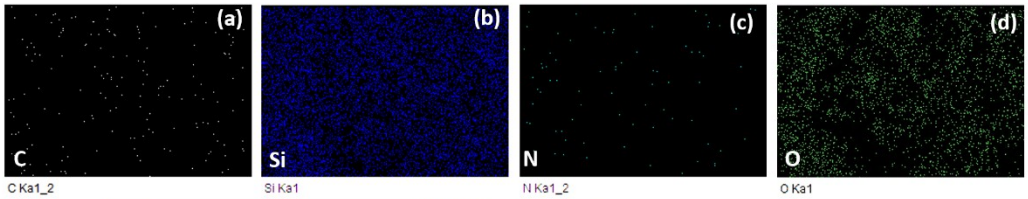

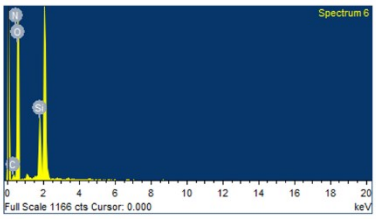

Element	Weight%	Atomic%
C K	8.55	11.67
O K	77.62	79.57
Si K	12.65	7.39
N K	1.18	1.38
Totals	100.00	

(ii)

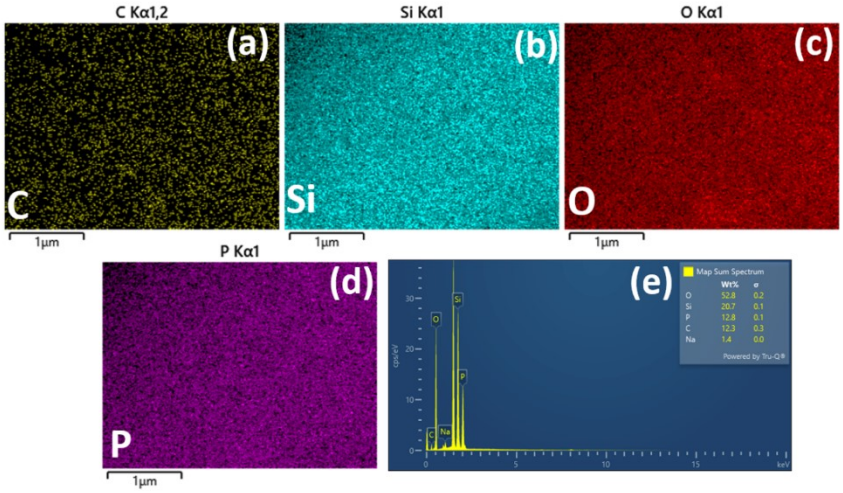

(iii)

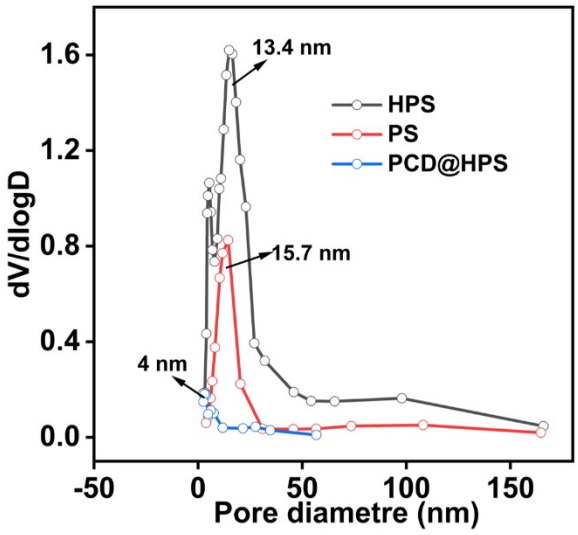

Figure S3: (i) SEM EDS of HPS showing (a) carbon, (b) silicon, (c) nitrogen, and (d) oxygen, and (d) EDS spectrum, (ii) SEM EDS of PCD@HPS showing (a) carbon, (b) silicon, (c) oxygen, (d) phosphorus, and (e) EDS spectrum, (iii) pore size distribution curve

Table S2: Parameters obtained from BET analysis

Sample code	BET Surface area (m^2/g)	Average pore diameter (nm)	Average pore volume (cm^3/g)
PS	339.4	15.7	1.05
HPS	72.69	13.4	0.31
PCD@HPS	4.7	4.6	0.09

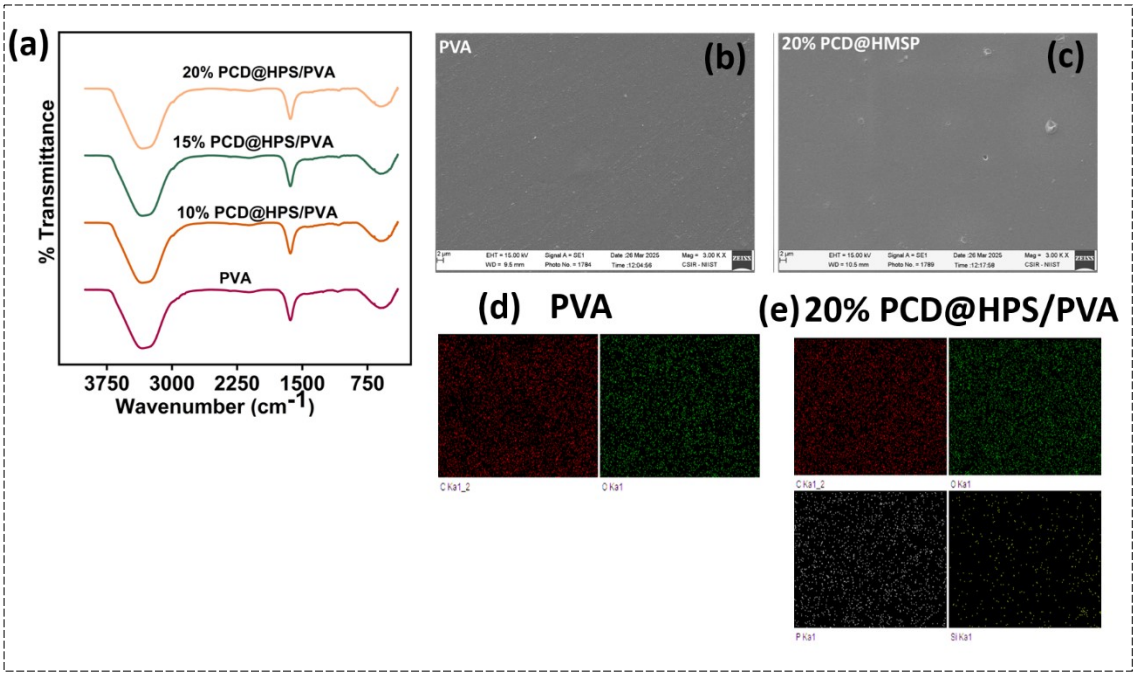

Figure S4: (a) Solution state IR spectra, SEM images (b)PVA, (c) 20% PCD@HPS/PVA, SEM EDS (d)PVA, (e) 20% PCD@HPS/PVA

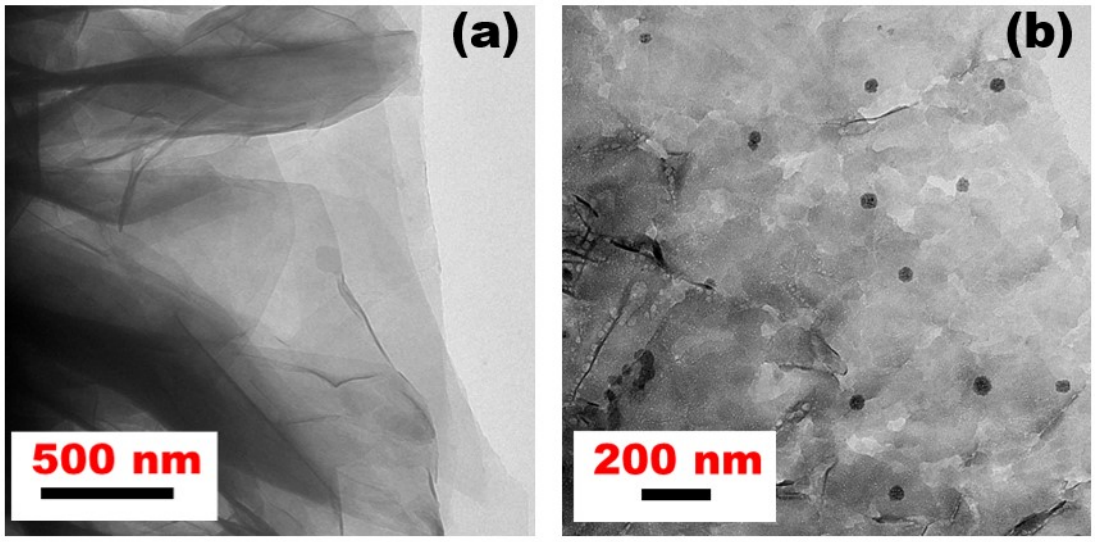

Figure S5: TEM images (a) PVA and (b) 20% PCD@HPS/PVA dispersions

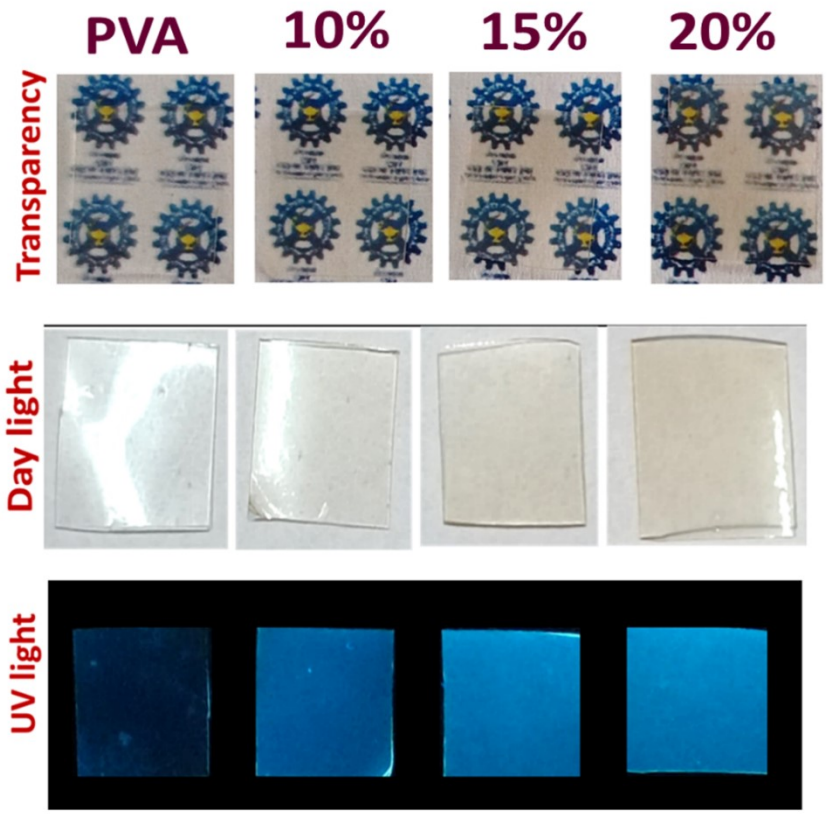

Figure S6: Physical appearance of films (a)Transparency, (b)Films under daylight, and (c) Films under UV light (365 nm)

Table S3: Color co-ordinates Whiteness (WI), yellowness index (YI), and transparency of PVA films

Samples	L*	a*	b*	Yellowness Index (YI)	Whiteness Index
PVA	96.58	0.03	0.35	0.51	98.02
10% PCD@HPS/PVA	97.33	0.06	1.57	2.3	94.9
15% PCD@HPS/PVA	96.8	0.08	2.2	3.24	97.2
20% PCD@HPS/PVA	94.63	-0.55	6.38	9.6	93.3

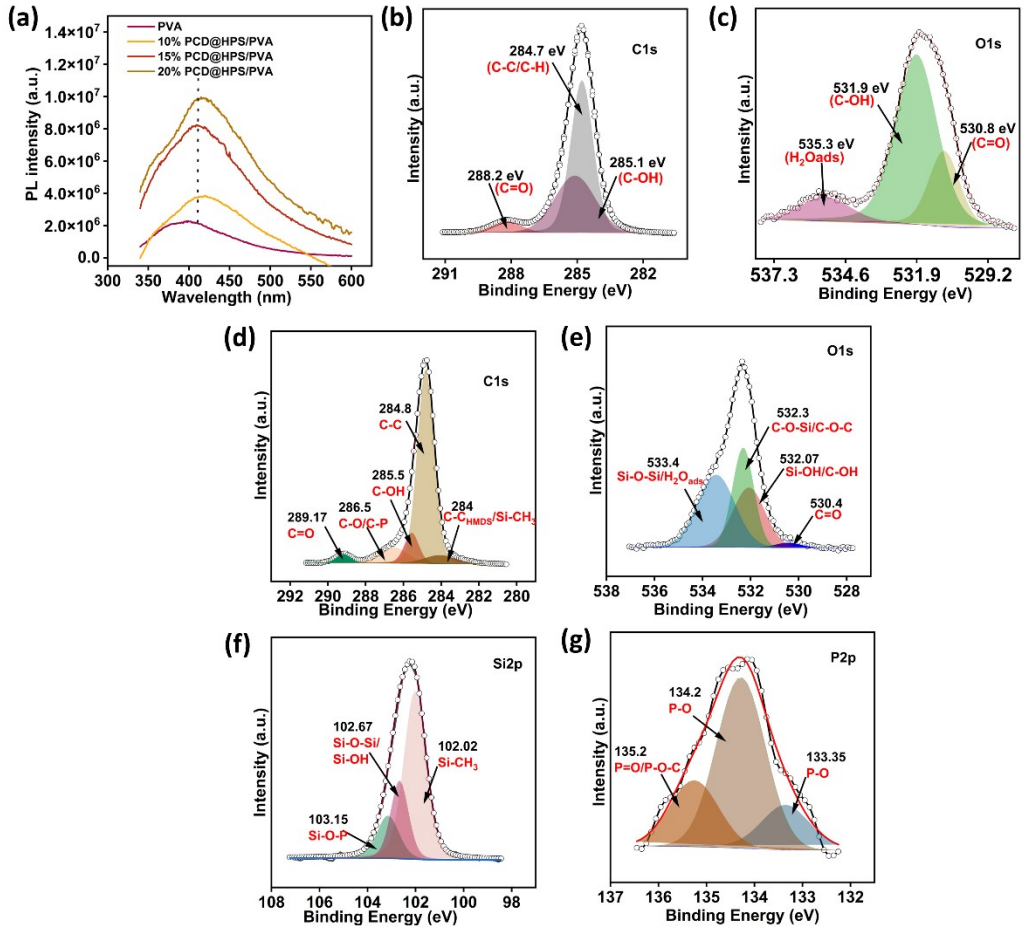

Figure S7: (a) PL Spectra of films, Deconvoluted XPS spectra PVA, (b)C1s, and (c) O1s, Deconvoluted XPS spectra of 20% PCD@HPS/PVA (d) C1s, (e) O1s, (f) Si2p, and (g) P2p

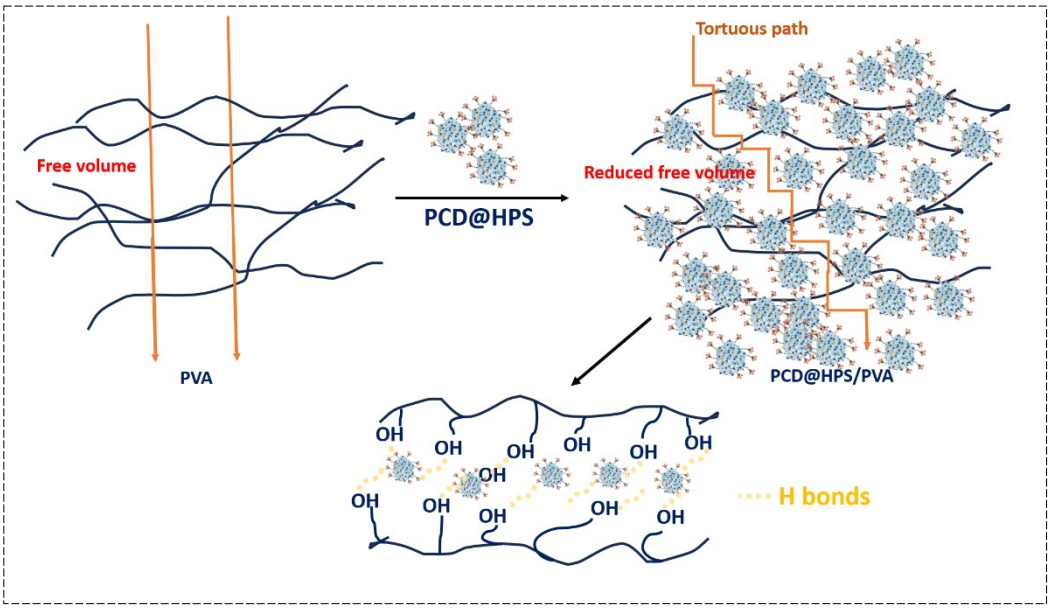

Figure S8: The influence of filler on the barrier property of PVA

Table S4: Comparison of barrier properties of the present study with recent literature reports

Material	**Thickness (µm)**	**OTR (cc /m²day)**	**WVTR**	**Barrier Mechanism**	**Reference**
Pure PVA	20	~7.29	-	Intrinsic polymer barrier	https://doi.org/10.3390/polym11030450
PVA	100	10	19.3		https://doi.org/10.1021/acsomega.3c02885
PVA / Graphene nanocomposite	100	~0.7	1.22	Tortuous diffusion pathway created by graphene sheets	https://doi.org/10.1021/acsomega.3c02885
PVA/ silica aerogel	61	~1.98	1.46	incensement of pathway for gas molecules passing through the film	https://doi.org/10.1016/j.lwt.2020.109568
PVA / PCD@HPS composite (This	**64**	**0.03**	7	Hybrid silica–carbon dot	**This work**

work)				tortuous pathway + strong interfacial interactions	

Table S5: Transmittance and transparency of the films.

Samples	**%T (UV-A) (315-400 nm)**	**%T (UV-B) (280-315 nm)**	**%T @ 280 nm**	**Transparency**
PVA	87.00	82.37	66	0.6
10% PCD@HPS/PVA	29.10	27.72	18.6	1.32
15% PCD@HPS/PVA	22.36	20.82	11.9	1.71
20% PCD@HPS/PVA	18.32	16.87	8	2.08

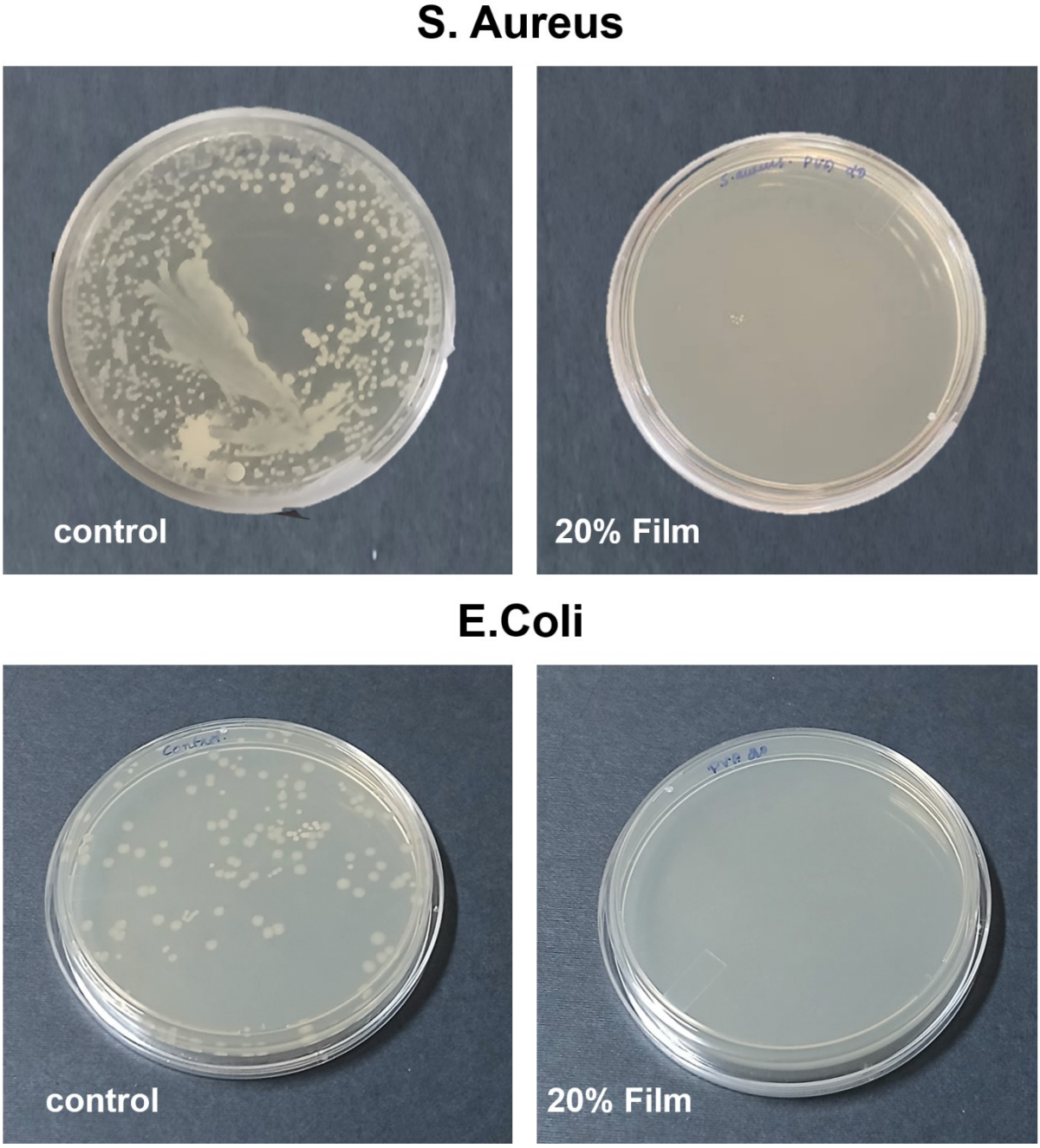

Figure S9: Antimicrobial Studies by Dynamic contact assay

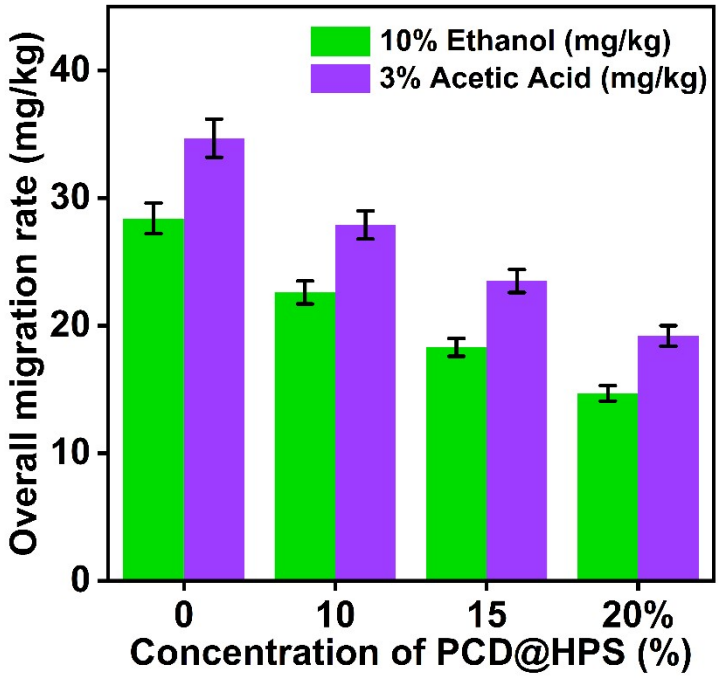

Figure S10: Overall migration rates of PVA and composite films in food stimulants

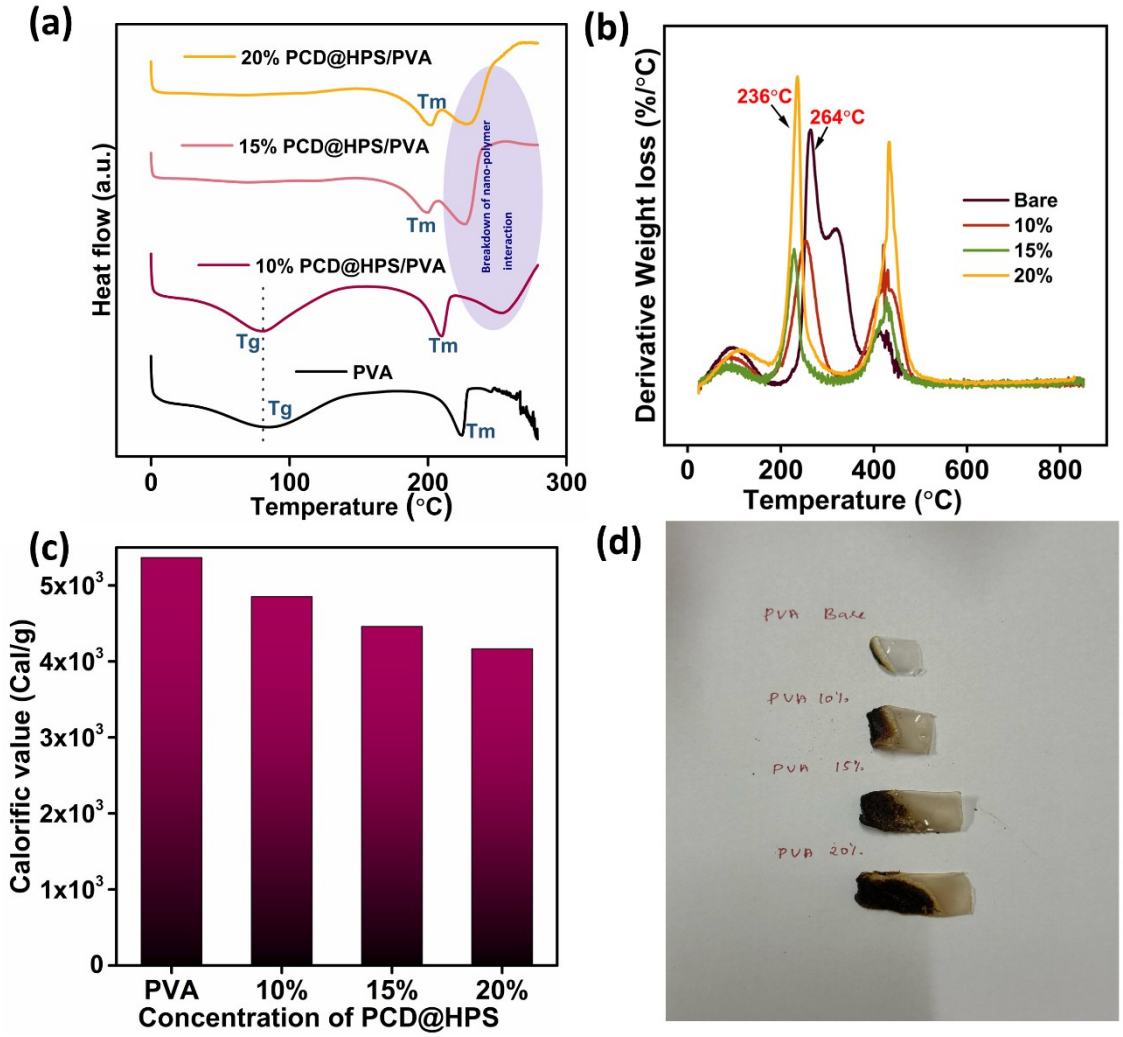

Figure S11: (a)DSC Spectrum of films, (b)DTG, (c) Bomb calorimetric values and (d) samples after the burning test.

Table S6: Thermal analysis of the films

Samples	$T_{5wt\%}$ (°C)	T_{max1} (°C)	T_{max2} (°C)	$Char_{700\,°C}$ (wt%)	LOI(%)
PVA	88	264	412	2.9	18.6
10% PCD@HPS/PVA	93	250	422	15.04	23.51
15% PCD@HPS/PVA	87	230	426	22.29	26.41
20% PCD@HPS/PVA	108	236	432	24.3	27.22

Table S7: Cone calorimetry data

Sample	TTI (s)	PHRR (kW/m^2)	TPHRR (s)	THR (MJ/m^2)	FGI (kW/m^2. s)	FPI ($s.m^2/kW$)	Av-EHC (MJ/ kg)
PVA	21.5	370.7	18	17.6	20.59	0.058	29.81
20%	23.25	174.7	11	9.7	15.88	0.133	24.14

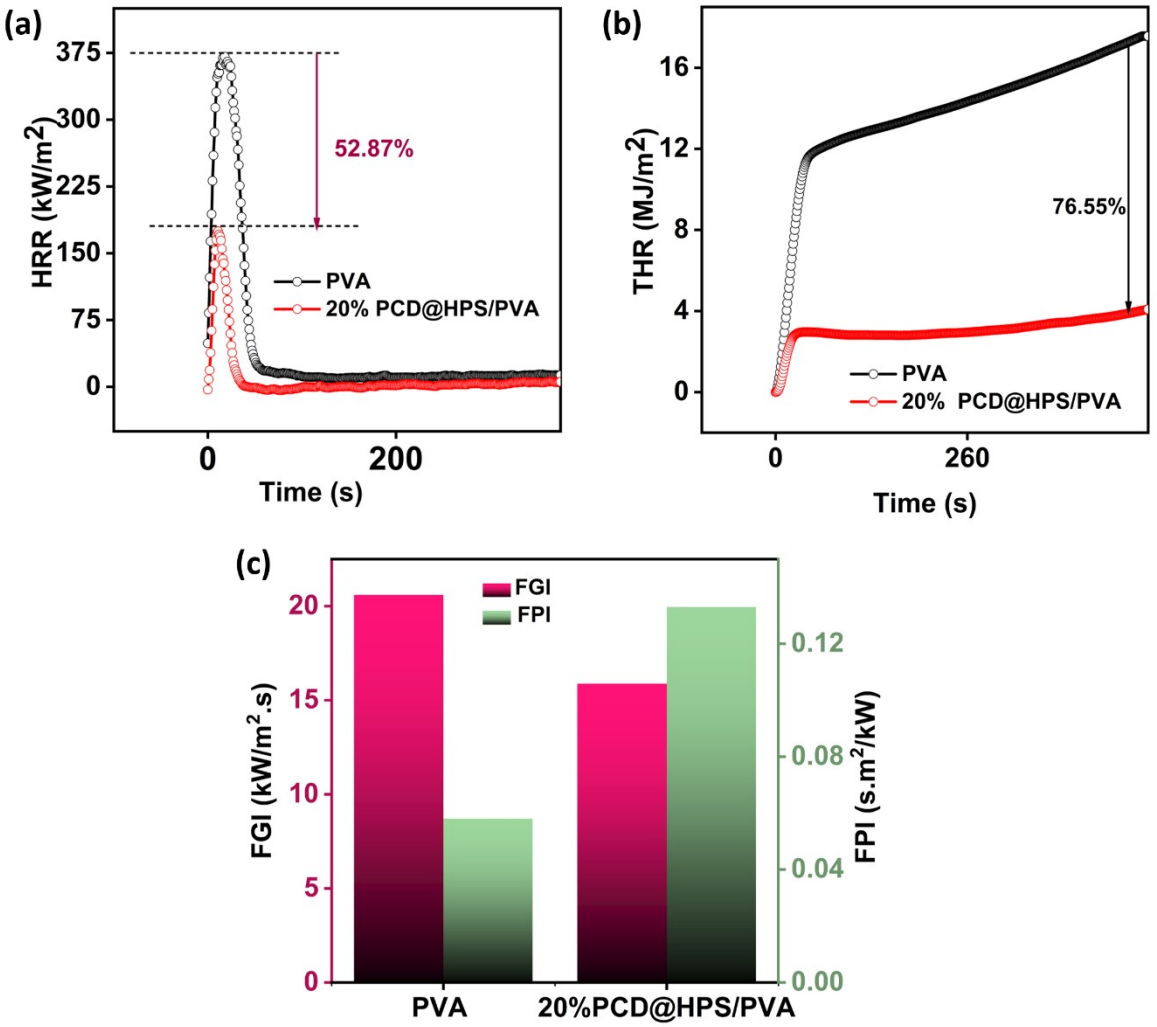

Figure S12: Cone calorimetric measurements (a) HRR, (b) THR and (c) FGI and FPI for PVA and 20% PCD@HPS/PVA

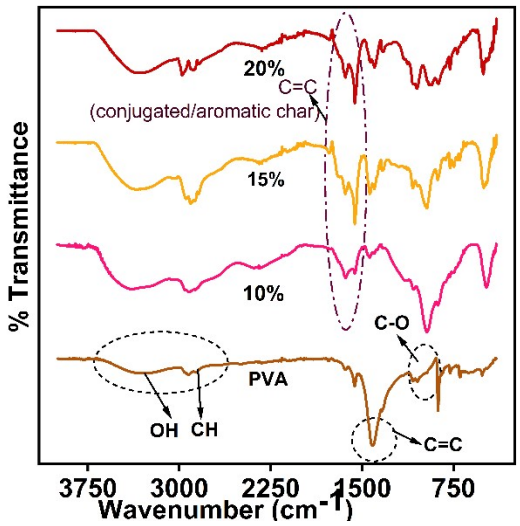

Figure S13: (a) IR spectrum

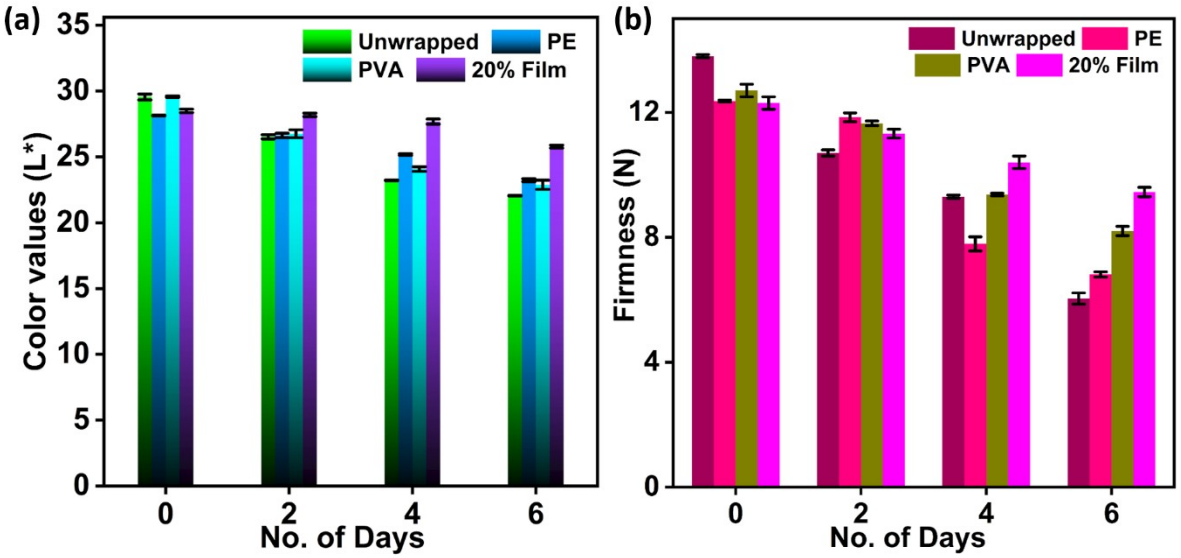

Figure S14: (a) Storage performance of strawberries (a) Colour (L*) and (b) Firmness

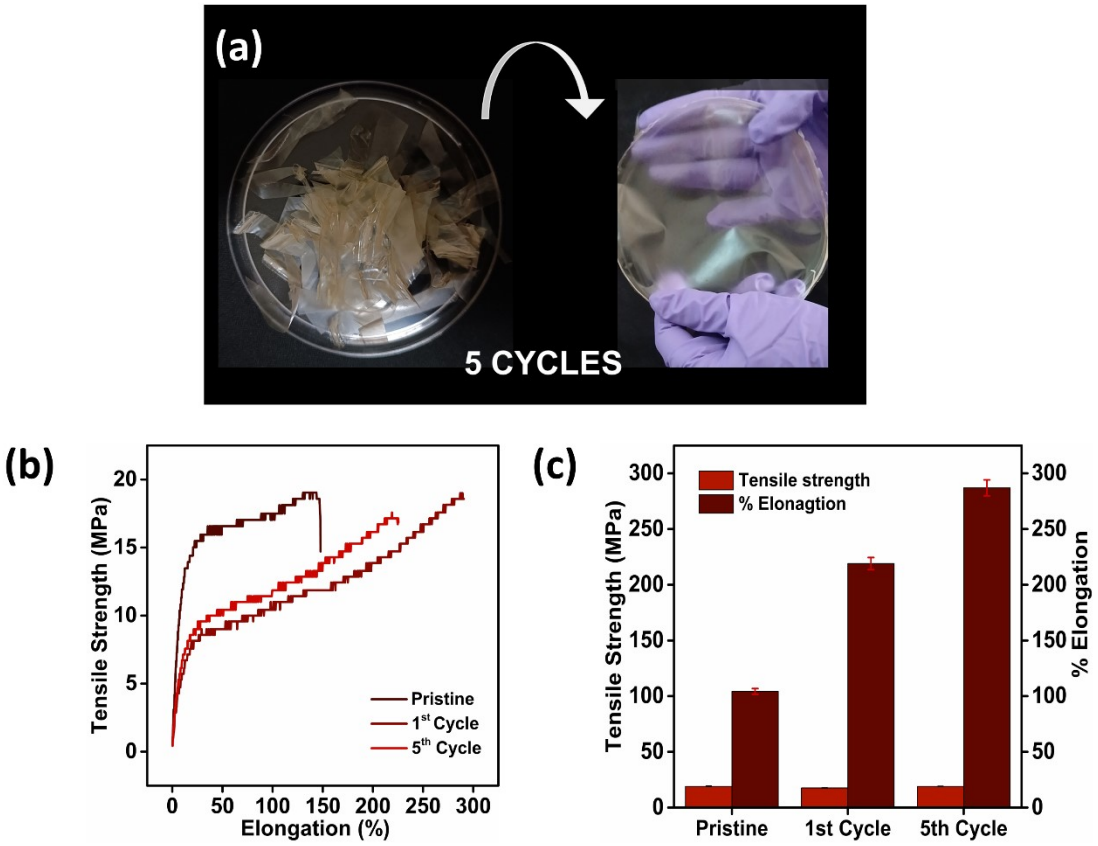

Figure S15: Reprocessability of 20%:film (**a)**) Digital images showing the recycling of the composite film for 5 cycles via solution casting, (**b**) stress-strain curves for the composite over first and fifth cutting/recycling cycles, (**c**)% elongation; Biodegradability analysis of PVA-based films under soil burial

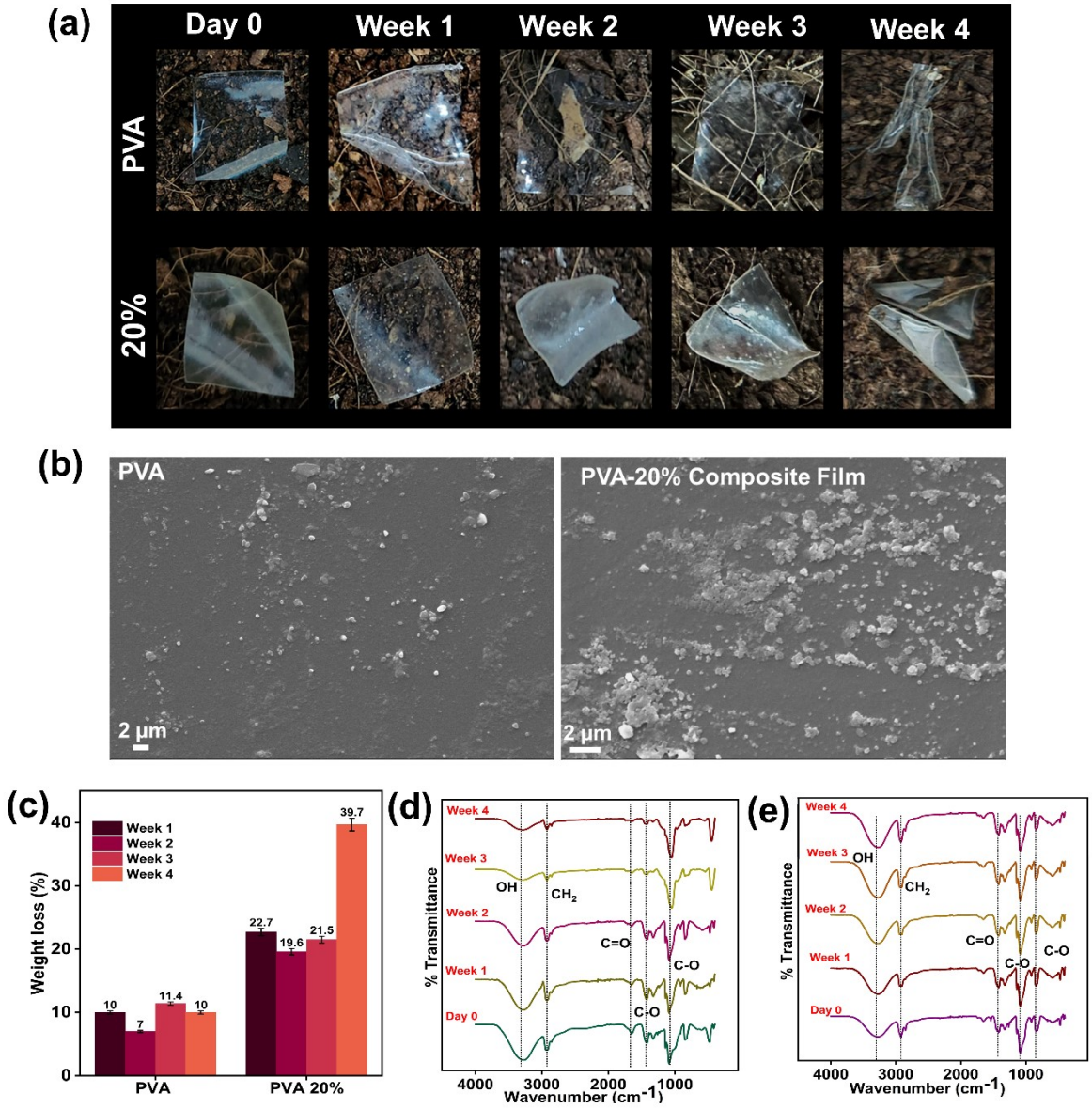

Figure S16: Soil burial test**(a)** digital images for visual appearance over 4 weeks, , **(b)** SEM images after 4 weeks for PVA and 20% film respectively, **(c)** corresponding weight loss measurements over time (**d**) FTIR spectra of PVA and (**e**) 20% films showing progressive changes in functional groups; demonstration of practical applications

Figure S17: Digital images showing a 20% film as carry bag

Table S8: Comparison of the present work with recent literatures

Filler	**Film thickness (µm)**	**CA (°)**	**WVTR ($g/m^2.day$)**	**OTR $cc/(m^2.day)$**	**LOI (%)**	**Mechanical properties**			**UV shielding (%)**	**Antibacterial properties**	**Biodegradability studies**	**recyclability**	**Ref with respect to main text**
						Tensile strength (MPa)	Toughness (J/cm^3)	% elongation					
Uncaria gambir (UG) extract-	39.9	-	-	-	-	65% Increment	:93% increment		100%	yes	-	-	1
PDA	150	85	high	high	40	26	35.5±1	205	yes	yes	yes	-	7
	100	-	-	-	31.0		33.18	294.33	yes	yes	-	yes	8
CDs		-	-	-	-	---			98.5%	yes			43

4-carboxybenzaldehyde (CBA)		67.3	-	-	-				-	-	yes	yes	45
Phophazene+chitosan+Cu		-	-	-	29.1	28.42		91.06		yes			23
sodium alginate and	80	-	109.2	-		87	-	-	yes		yes	-	13
Anthocyanin/chitosan	44	-	18.39 ± 0.18	3.185 ± 0.532 × 10−6		38.68 ± 0.87							51
MoS2-Ag-NCQDs	80		-	0.008 ± 0.00		78.92 ± 3.0	3000.93 ± 4.9	76.05 ± 1.0	83.5	-	-	-	48
grafted amino acid ionic liquids	-	-	-	-	30.1	-			-	-	yes	-	9
Zn-MOF@T-R	-	-	-	-	-	46% increment	-	-	73.2	yes	-	-	57
PCD@HPS	64	96	7	0.03	28	19.04± 0.47	2409±6	104±2	92	yes	yes	yes	**This work**

(1) Zhao, L.; Zhang, M.; Mujumdar, A. S.; Adhikari, B.; Wang, H. Preparation of a Novel Carbon Dot/Polyvinyl Alcohol Composite Film and Its Application in Food Preservation. *ACS Appl. Mater. Interfaces* **2022**, *14* (33), 37528–37539. https://doi.org/10.1021/acsami.2c10869.

(2) Sujon, Md. A. S.; Habib, M. A.; Abedin, M. Z. Experimental Investigation of the Mechanical and Water Absorption Properties on Fiber Stacking Sequence and Orientation of Jute/Carbon Epoxy Hybrid Composites. *J. Mater. Res. Technol.* **2020**, *9* (5), 10970–10981. https://doi.org/10.1016/j.jmrt.2020.07.079.
(3) Zhao, Z.; Xu, Y.; Zou, P.; Xu, L.; Cai, J. Developing a Pachyman/Polyvinyl Alcohol-Polylactic Acid Bilayer Film as Multifunctional Packaging and Its Application in Cherry Tomato Preservation. *LWT* **2023**, *186*, 115249. https://doi.org/10.1016/j.lwt.2023.115249.
(4) Liu, W.; Yu, W.; Wang, J.; Gao, J.; Ding, Y.; Zhang, S.; Zheng, Q. Enhanced Mechanical and Long-Lasting Antibacterial Properties of Starch/PBAT Blown Films via Designing of Reactive Micro-Crosslinked Starch. *Int. J. Biol. Macromol.* **2024**, *266*, 131366. https://doi.org/10.1016/j.ijbiomac.2024.131366.
(5) Amaregouda, Y.; Kamanna, K.; Gasti, T. Biodegradable Polyvinyl Alcohol/Carboxymethyl Cellulose Composite Incorporated with l-Alanine Functionalized MgO Nanoplates: Physico-Chemical and Food Packaging Features. *J. Inorg. Organomet. Polym. Mater.* **2022**, *32* (6), 2040–2055. https://doi.org/10.1007/s10904-022-02261-9.
(6) Fang, X.; Qing, Y.; Lou, Y.; Gao, X.; Wang, H.; Wang, X.; Li, Y.; Qin, Y.; Sun, J. Degradable, Recyclable, Water-Resistant, and Eco-Friendly Poly(Vinyl Alcohol)-Based Supramolecular Plastics. *ACS Mater. Lett.* **2022**, *4* (6), 1132–1138. https://doi.org/10.1021/acsmaterialslett.2c00283.
(7) Su, W.; Yang, Z.; Wang, H.; Fang, J.; Li, C.; Lyu, G.; Li, H. Synergistic Effect of Sodium Alginate and Lignin on the Properties of Biodegradable Poly(Vinyl Alcohol) Mulch Films. *ACS Sustain. Chem. Eng.* **2022**, *10* (36), 11800–11814. https://doi.org/10.1021/acssuschemeng.2c02290.
(8) Zhang, Y.; Jiang, F.; Zhao, W.; Fu, L.; Xu, C.; Lin, B. One-Pot Synthesis of Degradable and Renewable Cellulose-Based Packaging Films. *ACS Sustain. Chem. Eng.* **2022**, *10* (50), 16871–16881. https://doi.org/10.1021/acssuschemeng.2c05440.